A Chirp-based, Adaptive, Signal-dependent Reduced Interference Distribution for Limited Data

Yen Nguyen Thi Hong
University of Science and Technology
The University of Danang
Danang, Vietnam
nthyen@dut.udn.vn

Des McLernon
School of Electronic and Electrical Engineering
The University of Leeds
Leeds, UK
D.C.McLernon@leeds.ac.uk

Mounir Ghogho
School of Computer Science
International University of Rabat
Rabat, Morocco
m.ghogho@ieee.org

Linh Ho Duc Tam
University of Sciences
Hue University
Hue, Vietnam
Hdtlinh@hueuni.edu.vn

Syed Ali Raza Zaidi
School of Electronic and Electrical Engineering
The University of Leeds
Leeds, UK
S.A.Zaidi@leeds.ac.uk

Sami A Aldalahmeh
Faculty of Engineering and Technology
Al-Zaytoonah University of Jordan
Amman, Jordan
sami.dalahmah@gmail.com

***Abstract*—Noise-like artifacts, which are caused by incomplete and randomly sampled data, spread over the whole ambiguity domain, and thus seriously obscure the true time-frequency signature of the data. In this paper, a new design for the signal-dependent adaptive kernel is proposed, which is robust with missing data. The method relies on the properties of chirps whose auto-terms only reside in a fixed half of the ambiguity domain. The important thing is that this half excludes the Doppler axis, where the chirps' noise-like artifacts concentrate. By cutting out this region when performing the optimization problem, a better signal-dependent kernel for chirps is obtained, which efficiently suppresses not only the cross-terms but also the missing sample artifacts. Moreover, since any windowed non-stationary signals can be approximated as a sum of chirps, the proposed approach can be applied to other types of non-stationary signals. It is shown in the simulation that our method outperforms other reduced interference time-frequency distributions of incomplete observations.**

***Index Terms*—reduced interference time-frequency distribution, missing samples, signal-dependent kernel, chirps.**

I. INTRODUCTION

Time-frequency distributions (TFDs) are employed to analyze signals with time-varying spectral content in a wide variety of applications [1]–[7]. While numerous different time-frequency representations (TFRs) have been developed, no single time-frequency (TF) estimation is ideal in all cases. The most widely used method is the short-time Fourier transform (STFT), in which the Fourier transform is implemented for each sliding window to ascertain the signal 's frequency content [8]–[10]. The major limitation is the trade-off between time and frequency resolution. While the Wigner- Ville approach does provide better resolution, it suffers significantly from the cross-terms resulting from the bilinear product. This could lead to misinterpretation of local power location. To solve this problem, many approaches of signal-independent and signal-dependent reduced interference distributions (RIDs) have been proposed. The former involves applying a fixed two-dimensional (2D) low-pass filter in the ambiguity domain to capture the signal's auto-terms which normally locate around the center. However, these fixed masks do not always work effectively because there are signals with their cross-terms also residing near the origin and their auto-terms locating far away the center. As the distribution of cross- and auto-components in the ambiguity domain actually depends upon the analyzed data, signal-dependent kernels have been proposed to guarantee a good performance for a large class of signals. The radially Gaussian kernel (RGK) and its online performance version, adaptive optimal kernel (AOK), are outstanding examples in this category [11], [12]. In general, the algorithm of these signal-dependent kernels constructs a mask that automatically matches with the signal's auto-terms, and so it largely removes the cross-terms and performs well with many types of signals. However, in the case of missing samples, artifacts appear all over the ambiguity domain, which can be wrongly interpreted as signal auto-terms and misguide the conventional signal-dependent kernel methods to capture the incorrect region in the ambiguity domain, thus resulting in highly cluttered TFRs.

In this paper, we introduce a new design for the signal-dependent RID which can both efficiently remove cross-terms and combat with missing sample effects. The method relies on three features. Firstly, according to [15], a chirp's auto-terms always reside in only a fixed half of the ambiguity domain. Thus, for chirp signals, the other half of the ambiguity domain

Work of Mr Linh Ho Duc Tam was funded by Vingroup Joint Stock Company and supported by the Domestic Master/PhD Scholarship Programme of Vingroup Innovation Foundation (VINIF), Vingroup Big Data Institute (VINBIGDATA), code VINIF.2020.TS.95.

could be eliminated without any concern for loss of the signal's auto-terms. Secondly, the Doppler axis, where the chirp's artifacts gather, does not lie in the auto-terms residing half of the ambiguity domain. By removing the other half, the artifacts are largely suppressed. Finally, according to [13] and [14], any non-stationary signal segment can be approximated as a sum of chirps. Therefore, for any non-stationary signal segments, we can freely cut off the other half of the ambiguity domain. So this paper is organized as follows. Section II presents the artifact distribution of the compressed chirp signals, and the unsuitability of traditional signal-independent and signal-dependent RID in the case of incomplete data. Section III introduces the signal-dependent chirp-based adaptive kernels. Section IV shows simulation results. Finally, conclusions are given in section V.

II. COMPRESSED CHIRP SIGNALS

Denote $s(n)$ as the full chirp signal, which is expressed as follows:

$$s(n) = \exp\left[j2\pi\left(\alpha\frac{n^2}{2F_s^2} + \beta\frac{n}{F_s}\right)\right], \tag{1}$$

where α, β, F_s are the chirp rate, initial frequency, and sampling frequency, respectively. n is the discrete variable, $n = 0, 1, ..., N-1$, with N being the length of the signal. The corresponding instantaneous auto-correlation function (IAF) R_{ss} and ambiguity function (AF) A_{ss} are as follows [8]:

$$\begin{aligned} R_{ss}(n,b) &= s(n+\frac{b}{2})s^*(n-\frac{b}{2}) \\ &= \exp\left[j2\pi\left(\alpha\frac{nb}{F_s^2} + \beta\frac{b}{F_s}\right)\right], \end{aligned} \tag{2}$$

$$\begin{aligned} A_{ss}(\omega', b) &= \sum_n R_{ss}(n,b)e^{-j\omega' n/N} \\ &= \exp\left(j2\pi\beta\frac{b}{F_s}\right)\delta\left(\frac{\omega'}{2\pi} - \alpha\frac{b}{F_s}\right), \end{aligned} \tag{3}$$

where b, ω' are respectively the time lag and the Doppler angular frequency. Let us define $x(n)$ as the compressed data of the original full data $s(n)$, which is given as [16]:

$$x(n) = s(n)\left(1 - \sum_{n_m}\delta(n-n_m)\right), \tag{4}$$

where $n_m \in \{0, 1, 2..., N-1\}$ is a set of random time points when the original data is missing (i.e. set to zero) and $\delta(n)$ is the Kronecker delta function. The AF of the compressed data is written as:

$$A_{xx}(\omega', b) = \sum_{n=0}^{N-1} x(n+\frac{b}{2})x^*(n-\frac{b}{2})e^{-j\omega' n/N}. \tag{5}$$

With $x(n)$ in (4), the AF of the incomplete signal $x(n)$ obviously has four terms, which are the AF of the full signal $s(n)$ given by (3) and the three artifacts. The latter terms are denoted as V_1, V_2, V_3, and are expressed as follows,

$$V_1(\omega', b) = -\sum_{n'}\exp\left[j2\pi\left(\alpha\frac{n'b}{F_s^2} + \beta\frac{b}{F_s}\right)\right]e^{-j\frac{\omega' n'}{N}}, \tag{6}$$

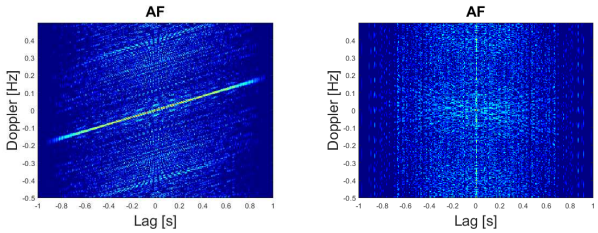

(a) (b)

Fig. 1: AF of (a) A compressed arbitrary chirp; (b) Four compressed arbitrary chirps.

$$V_2(\omega', b) = -\sum_{n''}\exp\left[j2\pi\left(\alpha\frac{n''b}{F_s^2} + \beta\frac{b}{F_s}\right)\right]e^{-j\frac{\omega' n''}{N}}, \tag{7}$$

$$\begin{aligned} V_3(\omega', b) = \sum_{n_m}\delta(b)\exp\left(-j\frac{\omega' n_m}{N}\right) + \\ \sum_{n=0}^{N-1}[R_{ss}(n,b)\sum_{n_m}\delta(n+\frac{b}{2}-n_m) \\ \sum_{n_l\neq n_m}\delta(n-\frac{b}{2}-n_l)e^{-j\frac{\omega' n}{N}}], \end{aligned} \tag{8}$$

where $n' = n_m - b/2$ and $n'' = n_m + b/2$. From (6), (7) and (8), it can be seen the missing data artifacts of a compressed chirp spread across the entire ambiguity domain. However, we should note that at $b = 0$, the total artifact at ω' is $V_1(\omega', 0) + V_2(\omega', 0) + V_3(\omega', 0) = -\sum_{n_m}\exp(-j\frac{\omega' n_m}{N})$ and this number will be many times larger if the signal is composed of more than one chirp. This is illustrated in Fig.1. Fig.1(a) shows that the entire ambiguity domain of a compressed chirp is seriously cluttered by artifacts, but their magnitudes are still less than that of the auto-terms. In Fig.1(b), when the signal is composed of four chirps and missing samples are present, the artifacts' magnitude along the Doppler axis gets stronger, and even overwhelms that of the auto-terms.

The above analysis discourages the use of traditional signal-independent kernels, which capture all values along $b = 0$ due to the marginal property. Besides, the chirps' auto-terms are not restricted to around the origin. By using the conventional signal-independent kernels, not only part of the chirp's auto-terms are omitted but also a major component of missing artifacts is passed through. The conventional dependent-signal kernel (RGK or AOK) is also not suitable to be applied in the case of incomplete signals, which is illustrated in Fig. 2. The artifacts along the Doppler axis ($b = 0$) are wrongly interpreted as the chirp's auto-terms and then the kernel will operate in favor of this region, taking all these terms (Fig. 2 (b)). This leads to highly contaminated TF representations (Fig. 2 (d)). So this paper proposes a new design approach to signal-dependent RIDs to provide robustness to compressed non-stationary signals.

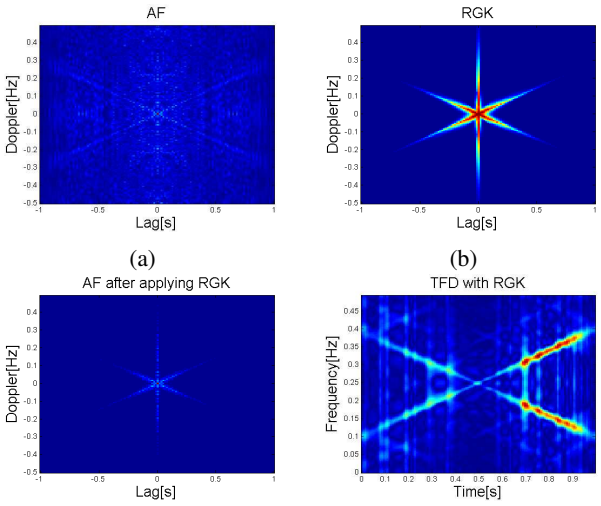

Fig. 2: (a) AF; (b) RGK; (c) AF after being filtered by RGK; (d) TFR with RGK for a signal composed of two crossing chirps. Note that 50% of the data is missing in all cases.

III. CHIRP-BASED ADAPTIVE KERNEL

A. Fixed signal-dependent kernel for chirps

This approach applies the chirp's properties in the ambiguity domain [15] and the algorithm of RGK to obtain a new kernel that is appropriate for chirps in the cases of full and incomplete data. The principle of RGK is that it keeps the magnitude of the kernel in the ambiguity domain large wherever that of the signal's AF is large, regardless of whether the peaks correspond to auto-terms or undesired terms ([11], [12]). This can be implemented by solving an optimization problem in the polar coordinates of the ambiguity domain, in terms of the radius r and the aspect angle ϕ. It samples the angle ϕ and the radius r into Q, and G discrete values, respectively. The original discrete Gaussian kernel in polar coordinates is then expressed as follows:

$$\begin{aligned} &C(g,q) = e^{-\frac{(g\Delta r)^2}{2\sigma(q\Delta\phi)^2}} \\ &g = 0,...,G-1,\ q = 0,...,Q-1, \end{aligned} \tag{9}$$

where g and q are respectively the radius and angle indices. Δr, $\Delta\phi$, and σ are the radius, the angle step sizes, and the spread parameter, respectively. Initially, the normal Gaussian kernel is used with equal spread parameter σ for every angle. Then, the spread parameter is updated by the gradient ascent method in such a way that it is large at a certain angle if the magnitude of the AF is large. The problem is that the magnitudes of missing sample artifacts along the Doppler axis are very strong, even larger then that of the auto-terms if the signal is composed of more than one chirp. Therefore, the RGK will be wrongly guided to take this region, which leads to noisy TFRs. Fortunately, for any chirps, the auto-terms always reside inside a half of the ambiguity domain, $|\phi| \leq \pi/4$ and $3\pi/4 \leq \phi \leq 5\pi/4$, which excludes the Doppler axis [15]. Therefore, the other half of the ambiguity domain can be removed without causing any loss of auto-terms. Furthermore, almost half of the cross-terms are removed. And more importantly, a major part of missing data artifacts is eradicated. Thus, the optimal kernel is modified so that the optimization problem is only carried out in the auto-term residing half of the ambiguity area. First, an edited version of the Gaussian kernel is applied in the ambiguity plane, where the spread parameter is zero outside the region $|\phi| \leq \pi/4$ and $3\pi/4 \leq \phi \leq 5\pi/4$. Then, the spread vector is updated by performing the optimization which is expressed as follows,

$$\begin{aligned} &\max_{C(n;g,q)} \sum_{g=0}^{G-1}\sum_{q=0}^{Q-1} r\,|A_{ss}(n;g,q)C(n;g,q)|^2 \\ &\text{subject to}\quad C(n;r,q) = \begin{cases} e^{-\frac{(g\Delta r)^2}{2\sigma^2(q\Delta\phi)}} & q\Delta\phi \in \mathbb{A} \\ 0 & else \end{cases} \\ &\qquad\qquad \sum_{q=0}^{N-1} \sigma^2(q\Delta\phi) \leq a, \end{aligned} \tag{10}$$

where a is the kernel volume ($1 \leq a \leq 5$) [11], [12], and $\mathbb{A}$ is the region of $|\phi| \leq \pi/4$ and $3\pi/4 \leq \phi \leq 5\pi/4$. The optimal kernel is converted to the coordinates of Doppler frequency and lag before being used to calculate the TF as follows,

$$TFD(n,k) = \sum_p \sum_b A(p,b)C(p,b)e^{-j2\pi np/N}e^{-j2\pi bk/N}, \tag{11}$$

where p is the discrete Doppler frequency, and k is the discrete frequency.

B. Chirp-based signal-dependent adaptive kernel

The above kernel is basically applied when the input signals are chirps and not for other types of non-stationary signals. Nevertheless, according to [14], [15], the frequency law of any non-stationary windowed signal can be approximated as a sum of chirps. Thus we can use the aforementioned fixed kernel for each windowed signal. The algorithm proceeds as follows. At each time n, we compute the short-time ambiguity function (STFT) centered at time n, which is given by:

$$\begin{aligned} AF(n;p,b) = \sum_u & s^*(u-b/2)w^*(u-n-b/2) \\ & s(u+b/2)w(u-n+b/2)e^{j2\pi up/N_w}, \end{aligned} \tag{12}$$

where $w(u)$ is a symmetrical window function which is zero when $|u| > N_w/2$. Then the signal-dependent kernel for the windowed signal, $C(n;p,b)$, is obtained by using (9). The current-time slice of the TFR is computed as follows:

$$\begin{aligned} &TFR(n,k) = \\ &\sum_p \sum_b A(n;p,b)C(n;p,b)e^{-j2\pi np/N_w}e^{-j2\pi bk/N_w}. \end{aligned} \tag{13}$$

IV. SIMULATION

This section evaluates the performance of the proposed chirp-based signal-dependent adaptive RID, with various types of non-stationary signals. The signals are sampled at the Nyquist rate, and then randomly shortened (as in (4)) to create the incomplete data to be processed. To get a visual comparison, the other three methods, Choi-Williams, the AOK, and the fixed chirp-based TFR [15], are simulated with the same signals. The resulting images are normalized and transfered to the energy versions to display. A parameter of concentration level ζ is used to access the accuracy of the resulting TFR. ζ is the ratio of the sum of pixel magnitude along the actual instantaneous frequency of the signals with respect to the rest of the TF values. So, the higher ζ, the more accurate the TF approximation. It is shown that our proposed method provides improved TF estimation. In all plots, the frequency axis is normalized with respect to the sampling frequency F_s.

1) Example 1: The first example considers a signal composed of a chirp and a sinusoid, which is given below:

$$s(n) = \exp\left\{j2\pi[(0.1F_s)\frac{n}{F_s} + (0.3F_s)\frac{n^2}{2F_s^2}]\right\} + \exp\left\{j2\pi[(0.1F_s)\frac{n}{F_s}]\right\} + v(n), \tag{14}$$

with the sampling frequency $F_s = 256$ Hz. The signal's length is one second, or $N = F_s$, and $n = 0, ..., N-1$. The signal is corrupted by white Gaussian noise $v(n)$ with the signal-to-noise ratio (SNR) set to 30 dB. The window size must be chosen carefully to ensure that the signal captured gives meaningful interpretation in time-frequency domain while it still can be approximated as a chirp. With signal length of 256, a rectangular window of length $N_w = 64$ is used. We randomly remove 50% of the signal samples to generate the compressed observations as in (4).

The resulted TFRs are shown in Fig. 3. The traditional fixed Choi-Williams kernel takes in all artifacts along the Doppler axis. It also cannot filter the cross-terms locating near the origin of the ambiguity domain. Thus, the TF signature is very contaminated with the concentration level $\zeta = 0.73$. The fixed windowed chirp-based kernel gives a better performance as can be seen in Fig. 3(c) because it suppresses more cross-terms and artifacts. The concentration level is $\zeta = 1.74$. Fig. 3(b) has many vertical lines in the TFR obtained by the AOK. These lines are impulses caused by components captured along the Doppler axis. However, it performs better than the two signal-independent kernels with $\zeta = 3.39$. By removing the artifacts along the Doppler axis, the proposed signal-dependent chirp-based adaptive kernel achieves the most reliable result among the four methods with $\zeta = 6$.

2) Example 2: The second example is a multi-component signal as follows:

$$s(n) = \exp\left\{j(0.15F_s)\cos(2\pi\frac{n}{F_s} + \pi) + j2\pi(0.25F_s)\frac{n}{F_s}\right\} + \exp\left\{j(0.15F_s)\cos(2\pi\frac{n}{F_s}) + j2\pi(0.25F_s)\frac{n}{F_s}\right\} + v(n). \tag{15}$$

Similarly, we set $SNR = 30$dB, $F_s = 256$ Hz, $N = 256$, $n = 0, ..., N-1$. A rectangular window of length $N_w = 64$ is used. The signal is also randomly shortened by 50%. The simulation results in Fig. 4 show that both fixed and adaptive kernels based on the chirp give a better performance than the traditional ones. It is evident that the windowed Choi-Williams distribution is severely influenced by the cross-terms and the artifacts, which can be seen in Fig. 4(a). The concentration level is $\zeta = 0.52$. The fixed chirp-based kernel gives better results compared with the fixed Choi-William kernel with $\zeta = 2.48$. Similar to example 1, the AOK experiences some vertical lines as the result of wrong areas captured in the ambiguity domain. The concentration level is $\zeta = 3.5$. The TF estimations get improved when the signal-dependent chirp-based adaptive kernel is used with $\zeta = 5.8$. The performance of the proposed algorithm will be less desirable in the case of lower SNR and more missing samples. Nevertheless, with near- range applications, these aforementioned values for SNR and missing samples are suitable. Moreover, in all cases, the proposed method outperforms the conventional reduced interference distributions for incomplete data.

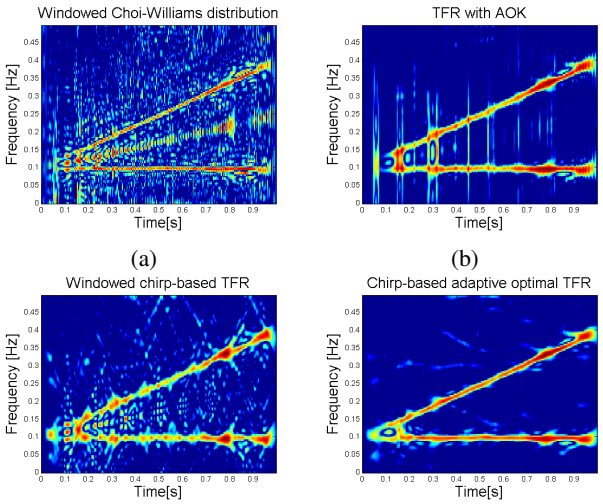

Fig. 3: Example 1, a chirp and a sinusoid with 50% data removed: (a) Windowed Choi-Williams distribution; (b) TFR obtained using the AOK; (c) Windowed chirp-based TFR; (d) Chirp-based adaptive optimal TFR.

V. CONCLUSION

This paper has introduced a new design for signal-dependent RIDs. Based on the fact that the auto-terms of chirps only

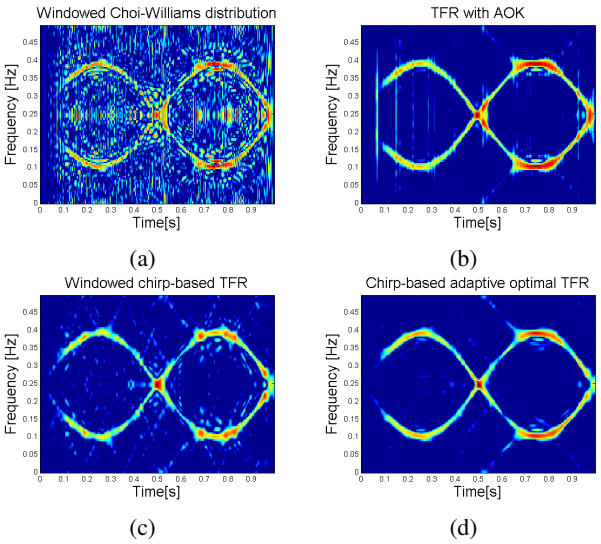

Fig. 4: Example 2, a multi-component signal with 50% data removed: (a) Windowed Choi-Williams distribution; (b) TFR obtained using the AOK; (c) Windowed chirp-based TFR; (d) Chirp-based adaptive optimal TFR.

reside inside a fixed half of the ambiguity domain, which does not accommodate the Doppler axis, and any non-stationary segments can be approximated by a sum of chirps, the proposed approach is operated on windowed signals with the kernel being zero outside that half of the ambiguity plane. By removing a half of the ambiguity plane where the signals' auto-term do not reside, the outcomes of the optimization problem are much better in the case of incomplete data as it does not wrongly capture the region of Doppler axis, where the artifacts always appear. Also, the kernel shapes in favour of the auto-terms and so that the cross-terms are efficiently suppressed. It is illustrated by simulations that our method is superior to other conventional signal-dependent and signal-independent methods when missing samples are present.

REFERENCES

[1] Chen, Victor C. The micro-Doppler effect in radar. Artech House, 2019.

[2] Chen, Victor C."Analysis of radar micro-Doppler with time-frequency transform." Proceedings of the Tenth IEEE Workshop on Statistical Signal and Array Processing (Cat. No. 00TH8496). IEEE, 2000.

[3] Setlur, Pawan, Moeness Amin, and Thayananthan Thayaparan."Micro-Doppler signal estimation for vibrating and rotating targets." Proceedings of the Eighth International Symposium on Signal Processing and Its Applications, 2005.. Vol. 2. IEEE, 2005.

[4] Stridh, Martin, et al."Sequential characterization of atrial tachyarrhythmias based on ECG time-frequency analysis." IEEE Transactions on Biomedical Engineering 51.1 (2004): 100-114.

[5] Christov, Ivaylo, et al. "Comparative study of morphological and time-frequency ECG descriptors for heartbeat classification." Medical engineering and physics 28.9 (2006): 876-887.

[6] Miwakeichi, Fumikazu, et al."Decomposing EEG data into space time–frequency components using parallel factor analysis." NeuroImage 22.3 (2004): 1035-1045.

[7] Yilmaz, Ozgur, and Scott Rickard. "Blind separation of speech mixtures via time-frequency masking." IEEE Transactions on signal processing 52.7 (2004): 1830-1847.

[8] Cohen, Leon. Time-frequency analysis. Vol. 778. Englewood Cliffs, NJ: Prentice Hall PTR, 1995.

[9] Daubechies, Ingrid. The wavelet transform, time-frequency localization and signal analysis. Princeton University Press, 2009.

[10] Choi, H-I., and William J. Williams. "Improved time-frequency representation of multicomponent signals using exponential kernels." IEEE Transactions on Acoustics, Speech, and Signal Processing 37.6 (1989): 862-871.

[11] Baraniuk, Richard G., and Douglas L. Jones. "A radially-Gaussian, signal-dependent time-frequency representation." IEEE International Conference on Acoustics, Speech, and Signal Processing (ICASSP). Vol. 5. 1991.

[12] Jones, Douglas L., and Richard G. Baraniuk. "An adaptive optimal-kernel time-frequency representation." IEEE Transactions on Signal Processing 43.10 (1995): 2361-2371.

[13] Nguyen, Yen TH, et al. "Time-frequency signature sparse reconstruction using chirp dictionary." Compressive Sensing IV. Vol. 9484. International Society for Optics and Photonics, 2015.

[14] Nguyen, Yen TH, et al. "Local sparse reconstructions of doppler frequency using chirp atoms." 2015 IEEE Radar Conference (RadarCon). IEEE, 2015.

[15] Nguyen, Yen Thi Hong, et al. "Time-Frequency Distribution for Undersampled Non-stationary Signals using Chirp-based Kernel." 2018 5th NAFOSTED Conference on Information and Computer Science (NICS). IEEE, 2018.

[16] Jokanovic, Branka, and Moeness Amin. "Reduced interference sparse time-frequency distributions for compressed observations." IEEE transactions on signal processing 63.24 (2015): 6698-6709.